Shot-earth for sustainable constructions

A. Curto[a], L. Lanzoni[b,c], A.M. Tarantino[c], M. Viviani[a]

[a] *HEIG-VD - Haute Ecole d'Ingénierie et de Gestion du Canton de Vaud, Route de Cheseaux 1, CH-1401 Yverdon*
[b] *DESD - Dipartimento di Economia, Scienze e Diritto, University of San Marino, Salita alla Rocca 44, Republic of San Marino, 47890 San Marino*
[c] *DIEF-Department of Engineering "Enzo Ferrari", University of Modena and Reggio Emilia, 41125 Modena, Italy*

Abstract

For centuries rammed earth has been used as building material and it is still used in many countries nowadays. On the other hand, excavated soil is becoming one of the largest construction waists that can be used as a construction material. A new type of rammed earth technology based on soil consolidation by spraying is presented in the present work. In particular, the working principle of the shotcrete is here extended to realize a new construction material called "'shot-earth"'. The base material is soil coming from excavation in construction sites. An experimental program has been carried out to characterize this new building material.

Keywords: Shot-earth; modern building materials; sustainable constructions.

1. Introduction

Even if in many countries soil has been replaced by others materials, it remains one of the most used construction materials for realizing houses and infrastructures. Many example of buildings constructed with soil have reached our era and stand to demonstrate that soil can be used as a durable construction material. The ancient city of Shibam (1a), the Tucson Mountain House (1b) designed by Rick Joy, the Wind-hover Contemplation Centre (1c) of the Stanford University and the M.Rauch's works, especially the Chapel

Email address: luca.lanzoni@unimo.it (L. Lanzoni)

of Reconciliation (1d), are some suggestive examples showing how soil can be a "user-friendly" material to realize sustainable constructions respecting the modern serviceability and security standards.

(a) Shibam "The Manhattan of the desert" in the 1930s

(b) Rick Joy won the Smithsonian Architecture Design Award with the Tucson Mountain House, Arizona, 2004

(c) Windhover Contemplation Center, Palo Alto, California

(d) The inside of the Chapel Of Reconciliation, Berlin, 1999

Figure 1: Recent constructions realized by using soil as building material

Based on an experimental investigation the present work shows that a common earth coming from excavation can be used as a construction material to realize structural as well as non-structural elements and for slopes consolidation. Particular attention is paid on the placing method. Conversely to the classical rammed earth compacted by mechanical devices, in this case the stabilized earth is placed using the same equipment used to spray the shotcrete. Such a technique takes advantage of the high speed at which the soil-gravel mixture is projected (the gravel serves to make compact the mix-

ture). This new construction material is named "*shot-earth*". The shot-earth used in this project is a "0 *km*" and "0 cost" material currently used in the same place where the soil is excavated to realize the foundation of the building. To date there are only few design criteria in Literature concerning earth constructions. Therefore particular emphasis is here paid to address the following issues: shot-earth as construction material; influence of the placing process on the earthcrete; earthcrete as construction technology. Reference is made to Switzerland rammed earth codes and the newest European Standards for concrete and masonry.
The experimental campaign consists of two main parts: the first one allows identifying the most important mechanical parameters such as ultimate compressive and tensile strengths, Young modulus and Poisson ratio. In the second one three walls have been realized to assess both the compressive and diagonal tensile (or shear) ultimate strengths.
The paper is organized as follows. The shot-earth technology is presented in Section 2, whereas Section 3 deals with the experimental campaign, with specific reference to the sample preparation according to standards. The evaluation of compressive strength has been presented in Section 4.1. The determination of the Young modulus and Poisson ratio is reported in Sections 4.2 and 4.3, respectively, whereas tensile strength has been evaluated as reported in Section 4.4. Realization and mechanical testing of wall samples has been reported in Section 5. Finally, conclusions are drawn in Section 6.

2. Shot-Earth Technology

Shot-earth consists of a dry mix of soil, cement and sand (size 0-8 mm) propelled through a spraying nozzle. Atomized water is injected just after the mixture leaking to hydrate the cement and promote cohesion.
Typical mix designed in shot-earth technology is 7/7/2 (7 soil, 7 sand and 2 cement) ratio by weight in the dry mixture. The mixture is pressurized into a properly designed machine and conveyed through the hose to the spraying nozzle by a high velocity air-stream. Water is added in around 3% (by volume) just at the nozzle to hydrate the dry mixture. Having right consistency allows avoiding the use of plasticizers and viscosity modifiers. Shortage of water will prevent an adequate compaction; on the other hand excessive water content gives a too liquid mixture that might not held in place properly. Two projection methods were tested, one overhead on a closed mould (see Figure 2b), one on a vertical surface with an angle of approximately 45° with

respect to the horizontal (see Figure 2a). The overhead method resulted in a less performing material probably due to aggregates rebound in a confined mould. Indeed the aggregates that haven't been blended to the mix remain inside the form-work, thus leading to segregation phenomena.

(a) Shot-earth frontally sprayed.

(b) Shot-earth sprayed from overhead

Figure 2: Different methodologies used.

Furthermore during the spraying precess a greater cloud of dust is generated not allowing the nozzle man to see inside the formwork. The overhead technique is therefore more interesting when used on large horizontal surfaces rather that unconfined molds. The head-on shot-earth has shown a greater mechanical performance without segregation phenomena. This technique produces less dust as compared to the overhead technique and that means improve the working environment. The machine used to shot the stabilized earth is a twin chamber machine, similar to the one showed in Figure 3a. This equipment is generally used to shot refractory materials, mixes of dry sand and cement; it is a so-called dry process machine and its production rate equals 10 m^3/hr. This type of dry spray machine is appreciated by practitioners because of its steady rate of feeding into the air stream. This feature allows maintaining a constant water cement ratio and a constant rate of shooting: an unsteady air stream and the ensuing pulsation effect might causes segregation problem with loss of strength of the material. The sprayed dry process has shown a dense flow delivery during pumping, good workability and spraying ability, greater strength gain during early stages. These

(a) Boulder Gun machine used for spraying

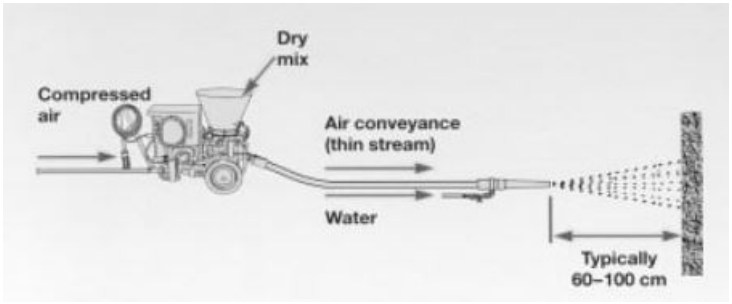

(b) Scheme of the Boulder Gun components

Figure 3: Designed machine for sprayed soil

certainly facilitates sealing and stabilization works at preliminary stages. The shot-earth is first placed into formwork and then finished by a steel float: this provides a smooth surface (see Figure 4c). The finishing process does not require additional water and finer is the aggregate used in the mix, easier is the smoothing process. Figure 4 presents the method used to manufacture structures with shot-earth. One of the characteristics of the shot-earth is the higher bonding with the substrate: the high air pressure with which the material is sprayed provides a sort of self compaction of the material. This allows placing the mix in the formwork without need further mechanical compaction. Indeed the self compaction plays a relevant aspect for reducing

(a) Specimen after spraying process (b) Specimen during finishing process

Figure 4: shot-earth spraying technology

segregation phenomena. This aspect definitely results in an increased quality of the mechanical performance of the material.

3. Experimental program

Materials used for the production of shot-earth specimens and the test methodologies are described herein. Owing to lak of specific methodologies aimed at characterizing shot-earth, the compressive strength and other parameters such as the Young modulus, Poisson ratio, shear modulus and tensile strength were determined by using standard tests for concrete and masonry [15], [22], [23], [24], [25], [26]. The experimental program consisted of two phases: the first one aimed at testing prismatic specimens; the second one devoted to investigate both axial and diagonal compression of walls samples. All specimens were cured at $23 \pm 1.7° \, C$ $(73 \pm 3° \, F)$ of temperature and $50 \pm 5\%$ of relative humidity and then tested at 28 days old. During the drying process the weight loss was monitored with the aid of a thermal camera.

3.1. Materials and preparation of the specimens

The first part of the experimental program was aimed to identify the mechanical properties by standard tests on specimens and in manufacturing and testing two walls. The particularity of the work herein highlighted is that the soil excavated from the site-work was directly used to manufacture

specimens and walls for the research purpose.

Basically soil used in construction should not have a greater organic matter content, therefore 25/50 cm of topsoil should be removed. In-situ soils require some processing such as drying, screening and sieving after use. Furthermore presence of pollutants should be checked carefully.

The mix design of the shot-earth was created using four components:

- **Soil**: the soil used to manufacture walls was constituted with a fraction of clay and silt less than 25%, and the coarser aggregates ,sand and gravel, greater than 50%. In general has the majority of particles ranging from 7 mm to 0.25 mm.
- **Sand 0/8**: the sand added was passed through a 8 mm gauge: the 90-99% of the total quantity, as the European Standard EN13139 on aggregates recommends.
- **Portland cement, CEM I 42.5 N**: is a pure portland cement (OPC [1]), consisting of least 95% in clinker; it's properties correspond to SN EN 197-1 standard. This cement type is suitable also for concrete with special requirements as shotcrete, mortar and underlay floors.
- **Water**: The water content is not greater than 3% (volume content) in order to avoid problem in the shooting equipments.

Table 1 lists the shapes and dimensions of specimens for each kind of test.

During the first experimental campaign two walls were manufactured. The shot-earth walls were designed with the approximate dimensions of $1000 \times 1000 \times 330$ mm^3. The solely difference between the two walls is the spraying angle with the wall surface. A wall was manufactured with stabilized soil frontally sprayed in an open formwork. The second was sprayed overhead in a closed formwork (as in rammed earth technique). The walls were matured for five months in varies climatic conditions and subsequently six cylindrical samples were taken by coring, as shown in Figure 5a.

[1] OPC: Ordinary Portland Cement

Test	$Cube[mm]$	$Cylinder[mm]$	$Prism[mm]$
Compression	$L = 150$		
Compression (coring from exsisting)		$\Phi = 150$ $H = 300$	
Flexural tensile			$W = 150$ $H = 150$ $L = 600$
Direct tensile (coring from exsisting)		$\Phi = 150$ $H = 300$	
Young modulus			$W = 120$ $L = 120$ $H = 360$
Poisson ratio	$L = 150$		

Table 1: Specimens dimensions. L = Length, Φ = diameter, H = Height, W = Width.

(a) Coring setup

(b) Segregation in shot-earth specimens

Figure 5: Coring setup and segregation phenomena.

The coring has shown visible differences in quality of the walls. The cylinders of stabilized soil sprayed from the top have shown segregation with separation of some size groups of aggregates in isolated locations with corresponding deficiencies of these materials in other location [27]. Figure 5b highlights this phenomenon.

Conversely, samples taken from the frontally sprayed wall had a greater compactness and strength, and their direct tensile and compressive strengths were measured by standard tests (as outlined in the section 4.1 and 4.4).

This first campaign confirmed that the distance and angle of shooting is capitally important to obtain both good mechanical performance and aesthetics qualities; that's why the overhead technique was gotten set aside for this type of structural element.

4. Testing on shot-earth

The Young modulus, Poisson ratio, compressive and tensile strengths play an important role in design of structures.
Many techniques are available to measure the previous parameters and some of these are standardized for materials such as concrete. One of most used test is the uni-axial loading of a specimen (compressive test described in

subsection 4.1) at a fraction of the compressive strength. Both Young modulus and Poisson ratio were evaluated using a uni-axial compression test by measuring longitudinal and transverse deformations.

4.1. Compressive Test

The compressive strength was determined by using the test procedure for the concrete. In fact this shot-earth mix has shown mechanical properties that resemble those of a low strength concrete.
The machine used for this test was the "Walter Bai" machine in Figure 6. The compressive test was carried out on five 15 x 15 x 15 cm^3 cubes cured 28 days old. These were placed between the load platens of the test machine, which was set in load control at 13.5 kN/s.

Figure 6: Compression test setup

The strength values are shown in Table 2. The table summarizes the compressive strength obtained from the above described test: it should be noted that σ_c showed a relatively low scattering because values varied between 8.258 and 10.373 MPa. In general the specimens have a brittle failure after achieving their maximum compressive stress, as seen in the diagram stress-strain (see Figure 7).
The crack pattern was characterized by the formation of a cone shaped, a failure mode admitted by codes.

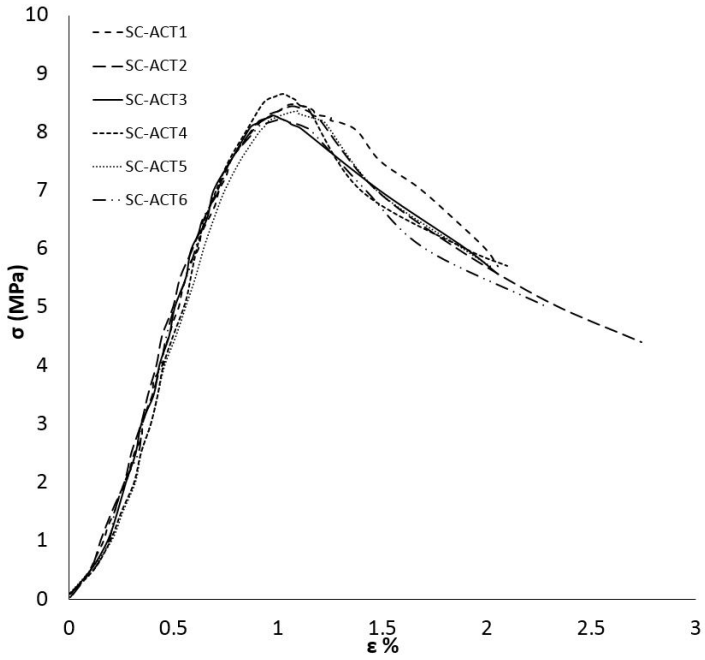

Figure 7: $\sigma - \epsilon$ behavior under compression

4.2. Young Modulus

Young modulus was determined according to EN 12390-13 [29]. The test method allows determining two moduli of elasticity: the initial modulus, $E_{c,0}$ measured at first loading and the stabilized modulus, $E_{c,s}$ measured after three loading cycles (see Figure 8). The strain determination were based on

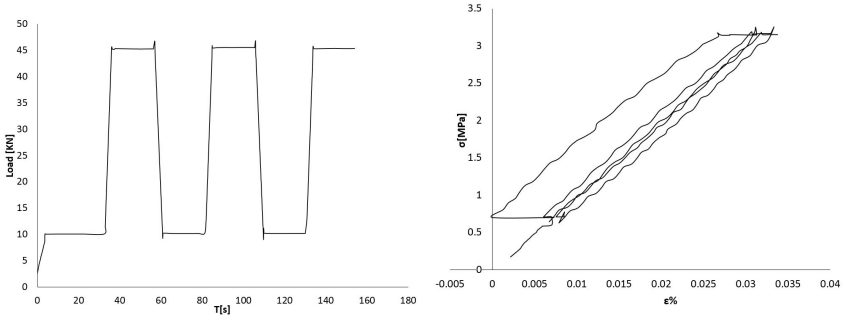

(a) Load-Time graphic (b) Stress-Strain cycles

Figure 8: Machine setting for Young modulus

Specimen	σ_c $[MPa]$
$SE-ACT1$	9.058
$SE-ACT2$	9.698
$SE-ACT3$	10.120
$SE-ACT4$	10.373
$SE-ACT5$	8.258
Average	9.501
$COV\%$	9

Table 2: Compressive strength

the ϵ curve, with three repetition of loading for measuring the time effect. The $E_{c,s}$ corresponds to the secant slope passing through the origin and to the ordinate point 0.33 σ_c [2].

$$E_{c,s} = \frac{\sigma_{1/3}}{\epsilon_{1/3}}$$

Results listed in Table 3 shown the stabilized Young modulus, which was computed between 5 and 33% of σ_c by linear fitting; it showed relatively low scattering and varied between 9638 and 11980 MPa; R^2 is the proportion of the variance in the dependent variable that is predictable from the independent variable(s). In Figure 9 stress-strain curves and the line of the linear regression are depict. The linear regression is a linear approach for modelling the relationship between scalars and the gradient of the trend line represents the Young modulus, $E_{c,s}(lr)$.

[2] σ_c: the mechanical compressive strength.

Specimen	$E_{c,s}$ $[MPa]$
$SE-YM1$	10521
$SE-YM2$	11980
$SE-YM3$	9638
$SE-YM4$	11793
$SE-YM5$	10639
$SE-YM5$	11366
$Average$	10990
$COV\%$	8
$E_{c,s}(lr)$	9707
$R^2\%$	88

Table 3: Young modulus; $E_{c,s}(lr)$: Young modulus by linear regression; COV% Covariance ; $R^2\%$ Coefficient of determination

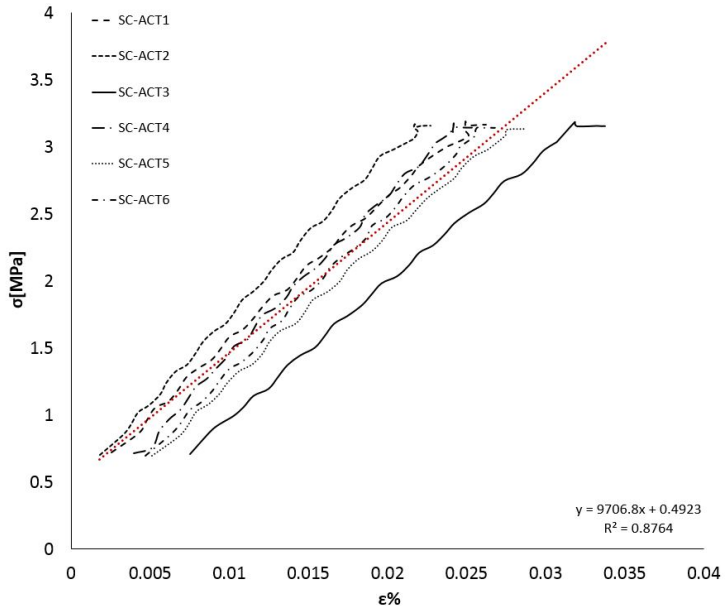

Figure 9: Stress-strain curves and trend line for Young modulus

4.3. Poisson coefficient determination

For evaluating the Poisson ratio, two transducers [3], orthogonally to the load direction and on the opposite cube sides were used for measuring the transverse strains; with comparing these to the longitudinal displacements, the Poisson ratio was evaluated,

$$\nu = -\frac{\epsilon_t}{\epsilon_l}$$

where ϵ_t and ϵ_l are the transversal and longitudinal strain, respectively. The strain transducers have a basis length of 75 mm (see Figure 10). The Walter Bay machine, with load cell of 200 kN, was connected to a terminal in turn connected to the two transducers; the system was set in displacement control with repetition of three cycles of loading and unloading (for the time effect) assuming to be in linear field and considering the range up to 0.33 σ_c. The system provided values for the load, longitudinal and lateral strains. The determined Poisson ratio are showed in table 4. It should be noted that ν showed high scattering because values varied between 0.1235 and 0.1815; actually is difficult to asses the Poisson ratio, because of the progressive breakdown of the specimen.

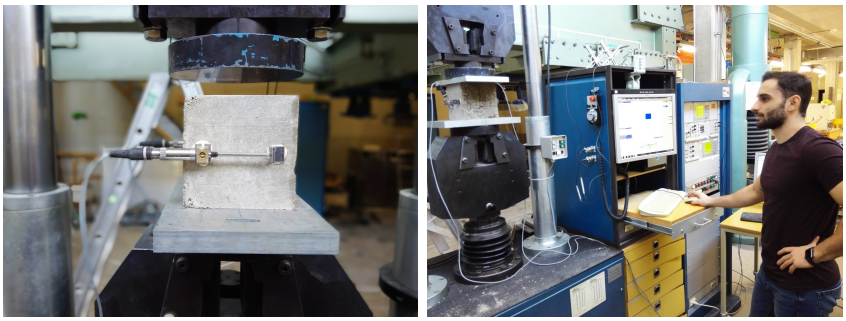

(a) Transducer disposition for the lateral strains

(b) Set-up machine

Figure 10: Machine setting to evaluate the Poisson ratio

[3] $\pm 1 \mu m$ of accuracy

Specimen	ν
$SE-PR1$	0.1588
$SE-PR2$	0.1235
$SE-PR3$	0.1815
Average	0.1546
$COV\%$	22

Table 4: Poisson ratio

4.4. Tensile strength

The tensile strength of shot-earth was measured with two different types of tests: direct and indirect methods.

4.4.1. Direct tensile test

The shot-earth has shown an elastic-brittle behaviour, thus the tensile branch may be described in detail with a linear constitutive law until the brittle failure according to the classical formula $\sigma_{ct}(\epsilon) = E_{ct}\epsilon$ in which E_{ct} is the elastic modulus of the tense soil-cement and ϵ is the axial strain. The direct tensile strength test consists of applying an increasing traction force until the failure of the specimen. Under the pure tension condition, the tensile strength value is measured as the ratio between load and specimen area and, compared with indirect methods, it gives more representative values than the flexural tests. Three shot-earth cylinders of 150 *mm* in diameter and 300 *mm* in height cored from existing wall, were tested under direct traction. The specimens were 5 months old and with compressive strength around 11 *MPa*. The middle cross section was reduced by 26% as shown in Figure 11. Table 5 summarizes mechanical properties of the shot-earth obtained from direct tensile tests. The average was found to be 1.159 *MPa*. Two extensometers with a gauge length of 38 *mm* were set to measure the longitudinal displacements.

The Figure 12 shows the stress-strain curve of the specimen under direct tensile test.

(a) Cross section reducing (b) Load application for direct tensile test

Figure 11: Direct tensile test set-up

4.4.2. Bending tensile test

In measuring the tensile strengths of brittle materials the direct method might be difficult, inaccurate and costly [33]. These are the reasons why the indirect tensile test is often carried out when a material is already well known. A typical three-point bending test [30] set-up is shown in figure 13. Maximum bending tensile stress is calculated under the assumption that the neutral axis is at mid-height of the cross-section and the stress distribution is triangular. The moment of inertia can therefore be approximated as $bh^3/12$ and the distance between the stress at the lower and the neutral line is

Specimen	$\sigma_{ct}[MPa]$
$SE-DT1$	1.057
$SE-DT2$	1.299
$SE-DT3$	1.120
Average	1.159
$COV\%$	10

Table 5: Direct tensile strength

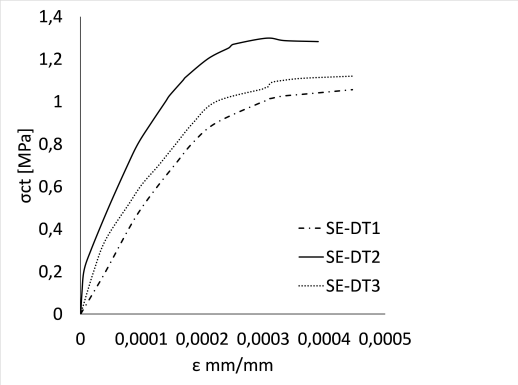

Figure 12: Stress-strain curve for direct test

Figure 13: Bending tensile test setup

$z = h/2$ [32]. The modulus of rupture, that is also defined as the bending tensile strength, can be measured using the classical formula:

$$\sigma_{ct} = \frac{M_{max}}{J_x} z = \frac{3FL}{2bh^2}.$$

Table 6 summarizes the flexural modulus of rupture of the shot-earth specimens. It should be noted that σ_{ct} shows relatively low scattering and varied between 2.281-1.759 *MPa*. Tensile strengths obtained by indirect ten-

Specimen	σ_{cft} $[MPa]$
$SE-BT1$	1.759
$SE-BT2$	1.993
$SE-BT3$	2.281
$SE-BT4$	1.817
$SE-BT5$	2.207
$SE-BT6$	2.165
Average	2.037
$COV\%$	11

Table 6: Tensile strength σ_{cft} provided by bending test

sile test is higher, by a factor of two or more, than those obtained by the conventional direct test [33].

4.5. Evaluation of experimental results

Analyzing the compression stress-strain diagram up to a third of the strength the behaviour can be considered linear elastic. At σ_c 70% of the maximum compressive strength the curvature increases rapidly (hardening) and, after achieving the maximum stress, the diagram shows a softening branch until the failure point, as depicted in the Figure 14. A certain loosening of the internal structure is shown after the 0.7 σ_c concomitantly with an increase of the transverse strain: this is an indication of the beginning of failure as a result of fatigue [**?**].

The measure of the tensile strength of soil-cement is dependent on the test used. The indirect tensile test has shown values conforming to the literature [**?**]: the ratio between tensile strength and compressive strength is 1 : 10.

As predicted, during the direct tensile test, failure of the three specimens occurred in the mid-section. Reduction of the cross-sectional area of the specimens resulted in increasing the stress in the middle of specimens, which induced a consistent failure.

The main characteristics of shot-earth are summarized in Table 7.

5. Walls Constructions and Testing

The data achieved from the first campaign on walls highlighted that the frontally spraying methodology yields best results. For the second exper-

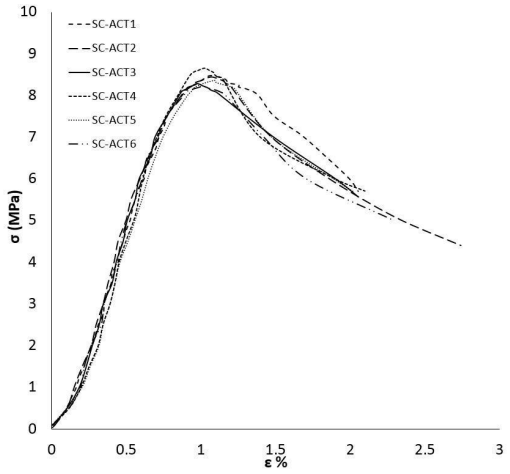

Figure 14: Rappresentative $\sigma - \epsilon\%$ behavior under compression

Type of test	*Average result*
Compressive strength, σ_c	9.501 $[MPa]$
Young modulus, $E_{c,s}$	9707 $[MPa]$
Poisson ratio, ν	0.1546
Direct tensile strength, σ_{ct}	1.817 $[MPa]$
Modulus of elasticity (direct tensile test), E_{ct}	2.207 $[MPa]$
Flexural strength, σ_{cft}	2.037 $[MPa]$

Table 7: Summary of testing result for shot-earth.

imental campaign on walls all the specimens were manufactured with the same shooting technique. Three walls were prepared and tested, two under axial compression and one under diagonal compression.

The two walls tested under compression were designed with the dimension of $800\times800\times100$ mm^3 and one of them was reinforced by a steel mesh in each side (see Figure 15). The third wall was manufactured with the dimension of $500\times500\times110$ mm^3 according to the ASTM E519/E519M-15, the standard test method for diagonal tension [25]. As shown in Figure 16, the drying process of the specimens was carried out at $20 \pm 2°C$ of temperature and $50 \pm 5\%$ of relative humidity (RH). The specimen weight was monitored using an electronic scale; the diagram weight-time is presented in figure 17. Over time the specimen lost around 6.4 kg of weight. This happened as a

Figure 15: Building site, Friburg, Switzerland

result of decreasing of the water content. To accurately measuring the bulk dry density, the specimen moisture was evaluated also using a thermocamera. The shot-earth wall manufactured have a bulk density of 2067.3 kg/m^3, a particle size range of about $0 \div 8$ mm and a shrinkage for both side of less than 0.5%.

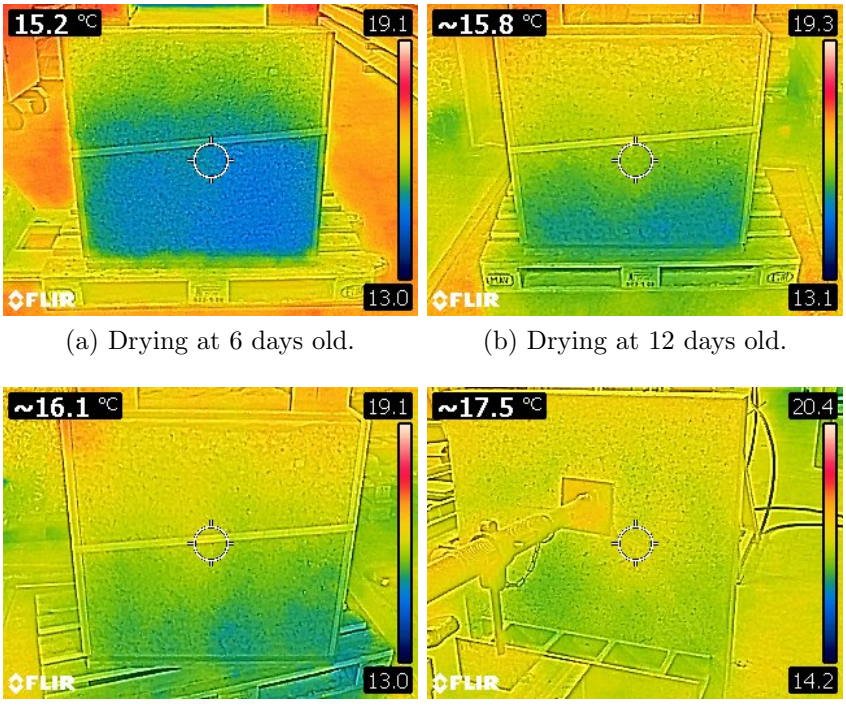

(a) Drying at 6 days old.

(b) Drying at 12 days old.

(c) Drying at 18 days old.

(d) Drying at 28 days old.

Figure 16: Drying process of the unreinforced wall

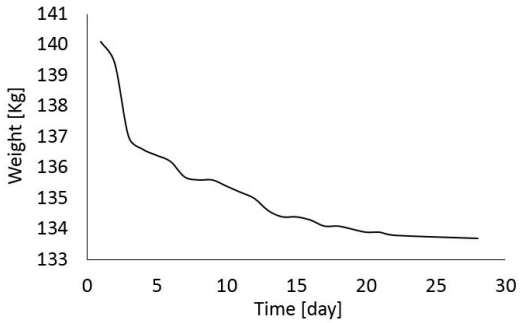

Figure 17: Drying process: relation between weight and time

5.1. Axial Compression Test

Before testing the walls under compression, the top surface was rectified by a rapid set cement mortar. The load applied to the specimen was distributed with a steel profile placed at the top surface. The machine system was set in displacements control with a speed of 0.6 *mm/sec*. The load is provided by four pistons with the maximum compressive load of 300 *kN* each; the load applied is measured by 3 button load cell (they are able to recording 500 *kN* each). Linear variable differential transducers (LVDT) with accuracy of 1 *mm* and the gauge length of 250 *mm* were placed on both faces of the specimen, for measuring the longitudinal and lateral displacements. The geometry of the supports and disposition of LVDTs is presented in Figure 18. The axial stress-strain curve (see Figure 19), for the unreinforced shot-earth wall, has shown an linear behaviour in the first part and then a progressive decreasing in rigidity until achieve the maximal load of 756.453 *kN*. The modulus of elasticity E equals 4418.7 *MPa* and it was computed on the range $5\% \div 30\%$ of σ_c. In general the wall exhibited a brittle failure in short time after achieving the maximum compressive stress. As depicted in the graph 19, the positive values represent longitudinal strain and the negative values represent transversal strain.

The reinforced wall was manufactured for the sole purpose of evaluate the shot-earth behaviour with steel reinforced in terms of technology application, workability and the interface soil-cement/steel. Regarding the reinforced wall, in fact, the failure occurred definitely without achieving the maximum compressive strength due to the concrete cover de-bonding. The axial stress-strain curve for the reinforced shot-earth wall (see Figure 20) is

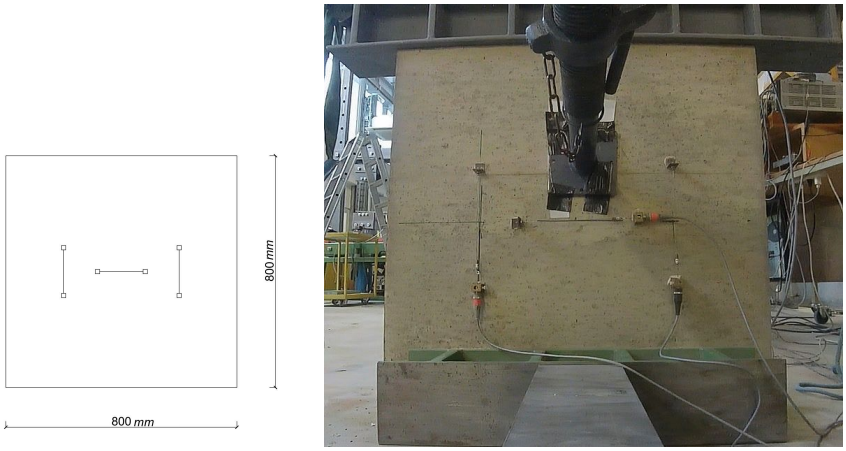

(a) Geometry of the LVDTs disposition

(b) Compression test

Figure 18: Geometry set-up and Linear variable differential transducers disposition

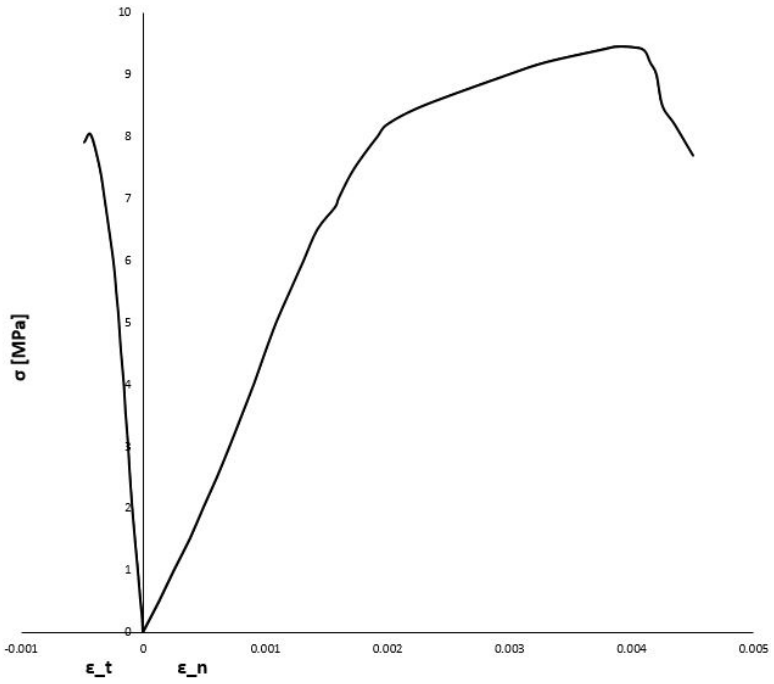

Figure 19: Stress-strain curve of unreinforced wall tested under compression.

still in the elastic branch with a Young modulus of 7406 MPa and with axial deformations in the range of $0.01 - 0.1\%$ before failure.

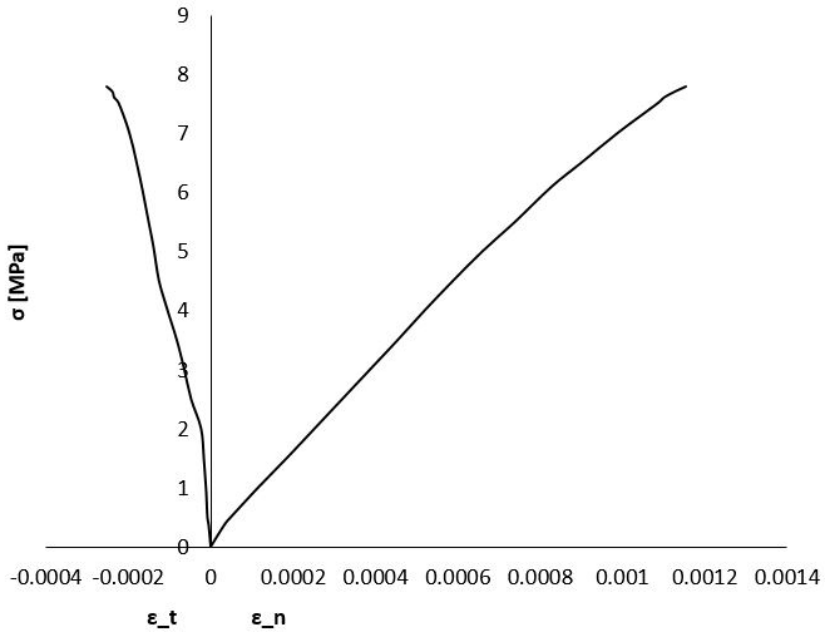

Figure 20: Stress-strain curve of reinforced wall tested under compression

	Unreinforced wall	Reinforced wall
F_c, maximum load $[kN]$	756.44	623.25
σ_c, compressive strength $[MPa]$	9.46	7.79
E, Young modulus $[MPa]$	4418.7	7406
ν, Poisson ratio	0.18	0.16

Table 8: Results of the axial compression test

Table 8 summarizes the mechanical properties of both walls tested under axial compression.In general the unreinforced walls evinced a brittle failure in a short time after achieving the maximum compressive load. Staying in the elastic field and comparing both walls, the reinforced wall has shown greater axial rigidity since the beginning of the test, and this high-lights that the steel reinforced could improve the shot-earth performance. Analysing the broken specimens it is evident that the shot-earth didn't has any problems to get through the steel cage and no segregation effect occurred (see Figure 21), even if the cage consisted in two layer of steel with 6 *cm* mesh.

5.2. Diagonal Compression test

This test method was developed to measure more accurately the diagonal tensile strength by loading the wall in compression along one diagonal, thus causing a diagonal tension failure with the specimen splitting apart parallel to the direction of load.
The diagonal compression test was performed according to the ASTM E519-15 [25]. The test set-up provides the layout of a compression load piston on the top surface with a maximum load of 300 *kN*. Two linear differential transducers (LVDT) were placed along the diagonals of both faces of the specimen as showed in Figure 22. The test was carried out under displacement control at 0.6 *mm/s*. The purpose of the diagonal compression test is to identify the shear mechanical parameters such as the ultimate shear strength τ, and the shear modulus G. While shear modulus measurements are considered accurate, the measure of the shear strength is complex. The presence of non-pure shear loading, non linear behaviour, edges, material coupling or the presence of normal stress makes shear strength determination questionable.

However,according to ASTM E519-15 standards [25] τ can be calculated

Figure 21: Reinforced wall failure

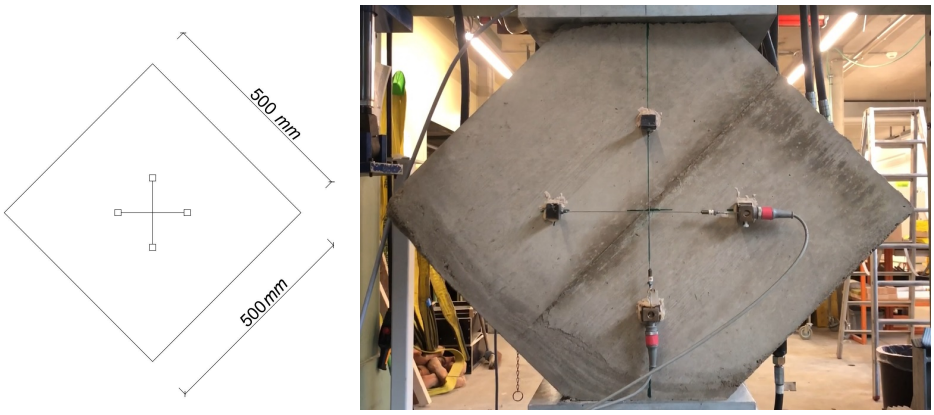

(a) Geometry of the LVDTs disposition

(b) Diagonal Compression test

Figure 22: Geometry of the test setup and LVDTs disposal

with the formula 1:

$$\tau = \frac{0.707P}{A} \tag{1}$$

being τ the shear stress, P is the load applied to the wall and A is the area of the specimen.

The shear strain is calculated as follows:

$$\gamma = \frac{\Delta v}{g} + \frac{\Delta h}{g} \tag{2}$$

where γ is the shearing strain, Δv is the vertical shortening, Δh is the horizontal extension and g is the gage length. Accordingly, the shear modulus turns out to be $G = \tau/\gamma$. Figure 23 depicts the shear stress-strain curve of the wall whereas Figure 24 shows the diagonal deformation during time.

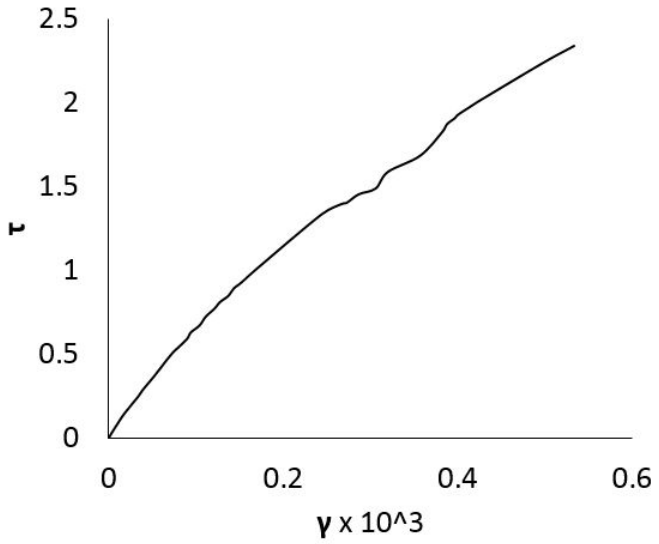

Figure 23: Shear-stress curve of a specimen under diagonal compression

	Specimen
P, maximal load $[kN]$	191.26
τ, shear stress $[MPa]$	2.45
G, shear modulus $[MPa]$	5981

Table 9: Results of the diagonal compression test

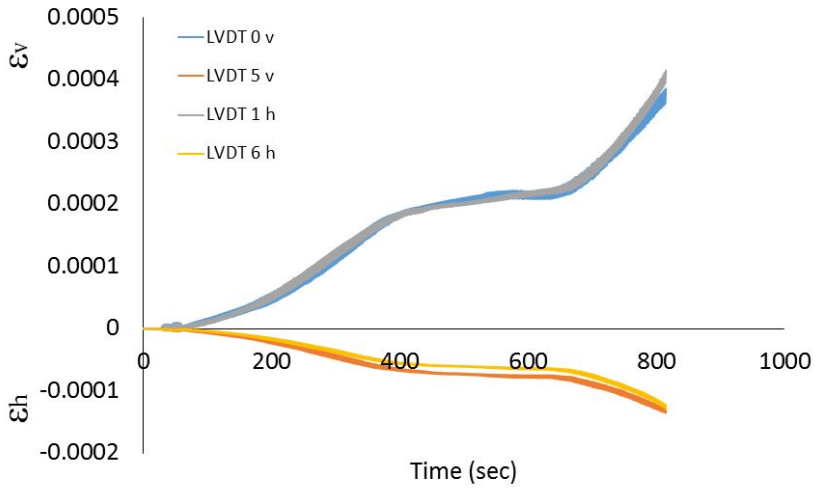

Figure 24: Strain-time curve of LVDTs

Table 9 showed the shear mechanical parameters. Assuming an elastic behaviour of the material, G was measured between the 5 and 33% of τ. The failure of the specimen was preceded by the appearance and consecutive propagation of a crack that crossed diagonally the specimen as showed in Figures 25a-b. Just before the failure a system of running cracks developed, causing the final failure.

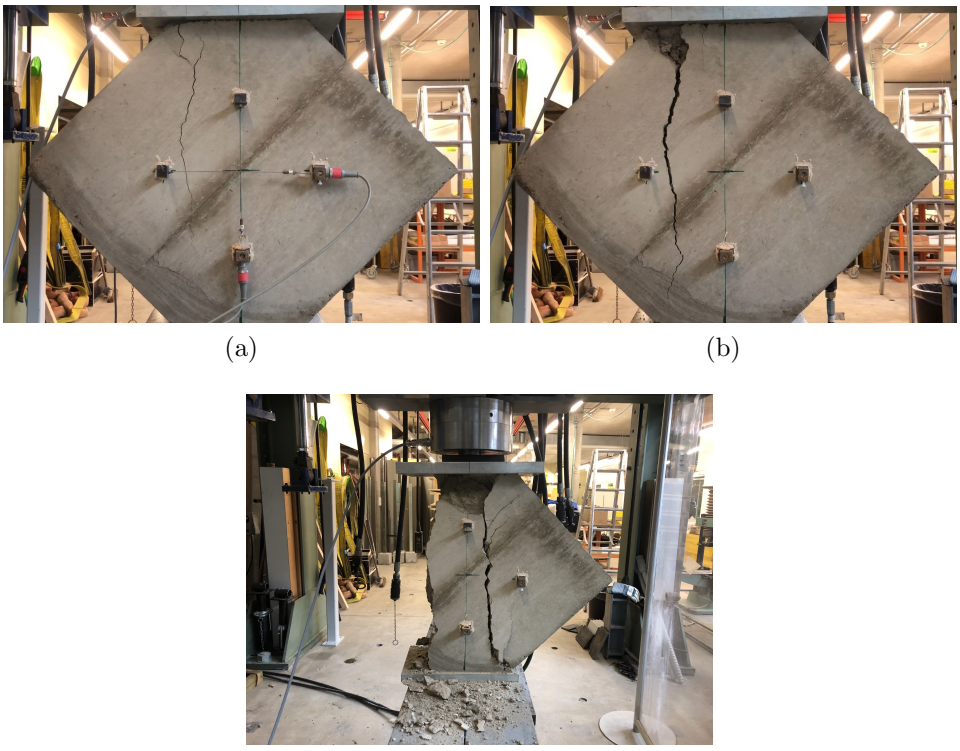

(a) (b)

(c)

Figure 25: shot-earth wall tested under diagonal compression cracks pattern

6. Conclusion

The shot-earth is a new construction material and consists in a mix of soil, sand and cement implemented by shotcrete technology. On the basis of the experimental program it might be argued that the mechanical behavior of shot-earth is similar to that of a low strength concrete. The experimental investigation accomplished in this work leads to the following conclusions:

- Excavated soil can be used as a construction material provided that its characteristics are known and a proper stabilization process is carried out;
- the principles valid for shotcrete hold also for shot-earth. This placing method allow a great homogeneity of the shot-earth and constant mechanical performances.

- based on experimental evidences the frontally methodology is suitable for the mix used, not only for increasing in mechanic performance, but also for the good workability and the self auto-compaction;
- the mechanical properties of shot-earth obtained with the 43% of soil are similar to those of a low-strength Portland cement concrete, as confirmed by several experimental tests.
- shot-earth may be considered as a green "0 cost" and "0 km" material and, in turn, it can be considered a sustainable material suitable for realizing green buildings.
- The use of shot-earth based on soil excavated in the same place where the soil is excavated leads to cost reduction in soil constructions manufacturing.

Further work will carried out to corroborate the results achieved in the present work. Such results are a prerequisite to properly calibrate the mechanical parameters which will be used in numerical modeling of structural elements. Since the shot-earth is used and it could be also used for many applications, such as slopes stabilization and pavements, further studies are also necessary on the interaction between this material and the environment, as well as on the shrinkage and creep.

Acknowledgements

Authors gratefully acknowledge the financial support provided by HEIG-VD. Financial support from the Italian Ministry of Education, University and Research (MIUR) in the framework of the Project PRIN *Modelling of constitutive laws for traditional and innovative building materials* (code 2017HFPKZY) is gratefully acknowledged.

Supplementary data

The raw/processed data required to reproduce these findings cannot be shared at this time due to time limitations. However the Authors will provide them soon.

References

[1] Cheng CT, Yang JC, Yeh YK. *Seismic performance of repaired hollow-bridge piers*. Construction and Building Materials, 17(5), 2003, 339-351.

[2] Lanzoni L, Nobili A, Tarantino AM. *Performance evaluation of a polypropylene-based draw-wired fibre for concrete structures*. Construct. Build. Mater. 28 (2012) 798-806.

[3] Lanzoni L, Tarantino AM. *Damaged hyperelastic membranes*. Int. J. Non-Linear Mech. 60 (2014) 9-22.

[4] Lanzoni L, Tarantino AM. *Equilibrium configurations and stability of a damaged body under uniaxial tractions*. ZAMP Zeitsc. Angew. Math. Phys. 66(1) (2015) 171-190.

[5] Lanzoni L, Soragni M, Tarantino AM, Viviani M. *Concrete beams stiffened by polymer-based mortar layers: Experimental investigation and modeling*. Construction and Building Materials 105 (2016) 321-335.

[6] Lanzoni L, Tarantino AM. *A simple nonlinear model to simulate the localized necking and neck propagation*. Int. J. NonLinear Mech. 84 (2016) 94-104.

[7] Nobili A, Lanzoni L, Tarantino AM. *Experimental investigation and monitoring of a polypropylene-based fiber reinforced concrete road pavement*. Construct. Build. Mater. 47 (2013) 888-895.

[8] Vanderwalle L. et al. Recommendation of Rilem TC162-TDF. *Test and design methods for steel fibre reinforced concrete. Design of steel fibre reinforced concrete using the s-w method: principles and applications*. Materials and Structures 2002;35:262-278

[9] ACI Committee 544. *ACI 544.4R88* Design consideration for steel Fiber Reinforced Concrete. ACI 544.4R-88America Concrete Institute. ACI Farmington Hills, MI 1996

[10] AFGCSETRA. *Ultra High Performance Fibre-Reinforced Concretes*. Interim Recommendations. AFGC Publication. France 2002

[11] CNR-DT 204. *Guidelines for design, construction and production control of fiber reinforced concrete structures*. National Research Council (CNR) of Italy 2006

[12] Deutscher Ausschuss für Stahlbeton (DafStb). *Guidelines for steel fiber reinforced concrete*. 23rd draft, richtlinie Stahlfaserbeton, DIN 1045 annex, parts 2007:1-4

[13] ACI Committee 318. *Report ACI 31808/318R-08*. Building code and commentary. Report ACI 318-08/318R-08 American Concrete Institute, Farmington Hills, MI, 2008

[14] UNI EN 206-1. *Concrete Part 1: Specification, performance, production and conformity* 2006

[15] UNI EN 12390-3. *Testing hardened concrete Compressive strength of test specimens* 2003

[16] UNI 11039-1. *Steel fibre reinforced concrete Definitions, classification and designation* 2003

[17] UNI 11188. *Steel fibres reinforced concrete structural elements Design, execution and control* 2007

[18] PrSIA 2052. *Béton fibré ultra-performant (BFUP)-Matériaux, dimensionnement et exécution* 2015-05

[19] UNI 11039-2. *Steel fibre reinforced concrete Test method for determination of first crack strength and ductility indexes* 2003

[20] Brite-Euram Project BRPRCT980813. *Test and Design methods for Steel Fibre Reinforced Concrete* 2001

[21] EN 1992-1-1. *Design of concrete structures General rules and rules for buildings* 1992

[22] UNI EN 12390-1. *Testing hardened concrete. Shape, dimensions and other requirements for specimens and moulds* 2012

[23] UNI EN 12390-5. *Testing hardened concrete. Flexural strength of test specimens* 2009

[24] UNI 6133. *Measuring the flexural tensile strength*

[25] ASTM E519/E519M-15. *Standard test method for diagonal tension (shear) in masonry assemblages*

[26] UNI 6135. *Standard test method for direct tensile strength*

[27] ASTM International 1956. *American Society for Testing Materials-Committee C-9 on Concrete and Concrete Aggregates (1 January 1956). Significance of Tests and Properties of Concrete and Concrete Aggregates*

[28] Hongxia Yang, 2012. *Experimental Study on Mechanical Property of Soil-Cement-Department of Civil Engineering, Shandong Jiaotong University*

[29] EN 12390-13. *Testing hardened concrete. Determination of secant modulus of elasticity in compression*

[30] ASTM-C293 2016. *American Society for Testing and Materials. International-Standard test method for flexural strength of concrete*

[31] Measurement of the tensile strength. *American Society for Testing and Materials A.R.C.S. R. BERENBAUM, Ph.D. and I. BRODIE. Measurement of the tensile strength of brittle materials. Mining Research Establishment, National Coal Board, Worton Hall, Isleworth, Middlesex, 9 October, 1958.*

[32] flexural strengths. *J.T.Balbo. Relations between indirect tensile and flexural strengths for dry and plastic concretes. IBRACON Estrut. Mater. vol.6 no.6, Dec. 2013.*

[33] Measurement of the tensile strength. *R. Berenbaum. Measurement of the tensile strength of brittle materials*

[34] ASTM E519-15. *Standard Test Method for Diagonal Tension (Shear),2015*

List of Figures